International Journal Of Scientific & Engineering Research, Volume 10, Issue 12, December-2019
ISSN 2229-5518

Exact 2D Thermo-Mechanical Stress Analysis of Exponentially Graded FG Laminate

Sandeep S. Pendhari[1], Sharawari P. Kulkarni[2]

Abstract-In this paper, two-dimensional (2D), heat-conduction equation has analytically solved. The aim of this is to determine an exact temperature field along with the thickness of simply supported laminate followed by stress analysis for thermomechanical loadings. Here, a two-point boundary value problem (BVP) has formed without any assumptions along with the thickness of a laminate, which is governed by a set of first-order ordinary differential equations (ODEs). A BVP has transferred to initial value problems (IVPs) by shooting approach, and the 4^{th} order Runga-Kutta-Gill numerical integration scheme has used during its solution. Young's modulus, heat conductivity, and coefficient of thermal expansion have been graded exponentially along with the thickness of a laminate. Poisson's ratio has held constant. Stress analysis has also performed for exponentially varied thermal fields through the depth of a laminate and compared with the structural response obtained for an exact variation of thermal field.

Index Terms: FG Laminate, Semi-analytical, BVP, PDEs, ODE, Thermomechanical, Exponential

1 INTRODUCTION

Functionally graded materials (FGMs) are first developed in Japan during the year 1984 for engineering applications, particularly in the thermal environment. As the name suggested, FGM is formed by the merely varying microstructure of constitutes form one point to other points. These are carried out with the help of specific functions, mostly by power-law or exponential-law, which helps to have the best benefits of different individual materials. Due to the gradual variation of volume fraction of ingredients, changes of specific material properties are smooth and continuous. These results in an un-offsetting variation in stresses at the lamina interfaces, which eliminates the inter-laminar stresses and considerably reduces the risk of delamination, which was associated with a layered domain. FGM mainly required where a very high thermal gradient. Which is to sustained over small material thickness, and therefore, thermal stress analysis of such materials is of most valuable.

Based on the Euler-Bernoulli theory (EBT), Sankar [1] presented an elasticity solution for simply supported functionally graded (FG) beams only for sinusoidal loading. Zhong and Yu [2] presented 2D analytical solutions based on Airy stress function for a cantilever beam with different boundary conditions and gradation laws. Higher-order flexural formulation, including wrapping and shear deformation effects presented by Benatta et al. [3]. Pendhari et al. [4] showed semi-analytical bending solutions for FG narrow beam subjected to transverse loads.
Comparative studies between the number of shear deformation theories have performed by Thai and Vo [5] to investigate the effect of the power-law index on the bending and free vibration responses of the FG beam. Influence of material length scale parameter, different material compositions, and shear deformation modes on static and free vibration analyses of FG micro-beam have been investigated by Simsek and Reddy [6] by adopting a size-dependent unified beam theory. Mostly, FG materials need to withstand an extreme thermal environment. Noda [7] has determined the optimum gradation laws for which the thermal stresses to be minimum. A closed-form solution developed by Sankar and Tzeng [8] for FG beams by varying thermo-elastic coefficients as well as temperature field along with the depth of beam according to exponential gradation. Analytical modes based on classical beam theory (CBT) and shear deformation theory have presented by Carpentari and Paggi [9] and Kadoli et al. [10], respectively, for thermo-elastic stress analysis of FG beam subjected to ambient temperature. Thermal buckling and thermo-elastic vibration response of FG beams graded according to power-law by using third-order shear deformation theory have reported by Wattanasakulpong et al. [11]. Nazargh [12] has documented thermal stress analysis of FG beams graded along with two directions for a thermal field, which is approximated by Hermite interpolation along with the depth of the beam. Apetre et al. [13] presented comparative studies for FG sandwich beams based on first, third, and higher-order shear deformation theories as well Fourier-Galerkin method. Numerical solutions for FG structures subjected to thermal and mechanical loadings have developed by Chakraborty et al. [14] and Carrera et al. [15]

- *Sandeep S. Pendhari* Associate Professor, Structural Engineering Department, Veermata Jijabai Technological Institute, Matunga, Mumbai 400 019, India, E-mail: sspendhari@st.vjti.ac.in
- *Sharawari P. kulkarni* Research Scholar, Structural Engineering Department, Veermata Jijabai Technological Institute, Matunga, Mumbai 400 019, India. *E-mail: sharawari2005@gmail.com*

International Journal Of Scientific & Engineering Research, Volume 10, Issue 12, December-2019
ISSN 2229-5518

based on finite element (FE) methodology and by Wang and Qin [16] based on meshless methods. Buckling studies of FG beam graded according to power-law when subjected to the thermal loads has demonstrated by Kiani and Eslami [17] based on Euler's Bernoulli theory. Thermo-mechanical solution based on the unified formulation for FG monolayer, as well as the sandwich beam, has discussed by Giunta et al. [18].

An effort has put here for the development of a semi-analytical model with the help of Fourier's law and partial differential equation (PDE) of heat conduction. These are carried out to obtained exact variation of temperature field through the thickness of FG laminates followed by thermal stress analysis for actual and exponentially assumed varied temperature fields. Developed mathematical models consist of the formation of two-point BVP governed by a set of coupled first-order ODE's (1) within the thickness of the laminate.

$$\frac{d}{dz} y(z) = A(z) y(z) + p(z) \tag{1}$$

Here $y(z)$ is an n-dimensional vector of primary variables whose number (n) equals the order of PDE. For heat conduction formulation, 'n' is equal to two, whereas, for stress analysis, it is similar to the four. $A(z)_{(n,n)}$, a coefficient matrix (a function of material properties in the thickness direction), and $p(z)$ is an n-dimensional vector of non-homogenous (loading). It is to note that loading terms include only body loads such as inertia loads, thermal loads, electric loads, etc. Surface loads have incorporated into the formulation during the solution procedure.

2 MATHEMATICAL FORMULATIONS

Consider a single layer of thickness 'h,' an FG beam of length 'a' along 'x' direction or FG plate of range 'a' along 'x' direction with infinite extent along 'y' direction. FG beam/plate is supported at two opposite edges (x=0, a) and subjected to mechanical and thermal loading, which varies only along with the length 'a.' Under such conditions, laminate is in plane-stress or plane-strain condition of elasticity in the x-z plane (fig. 1). Elastic modulus (E), coefficient of thermal expansion (α) and coefficient of thermal conductivity (λ) have varied only through the thickness of laminate accordingly to exponential law as,

$$E(z) = E_b e^{-In\left(\frac{E_b}{E_t}\right)z} ; \alpha(z) = \alpha_b e^{-In\left(\frac{\alpha_b}{\alpha_t}\right)z} ; \lambda(z) = \lambda_b e^{-In\left(\frac{\lambda_b}{\lambda_t}\right)z} \tag{2}$$

Here, subscript b and t defined the respective material properties at the bottom and top surface of laminates, respectively. Further, it assumed that the FG material is isotropic at every point, and Poisson's ratio is considered as kept constant throughout the domain. It is to point out that Kantrovich and Krylov [19] approach used in present formulations to transfer governing partial differential equation (PDE) to a set of coupled first-order ordinary differential equations (ODEs).

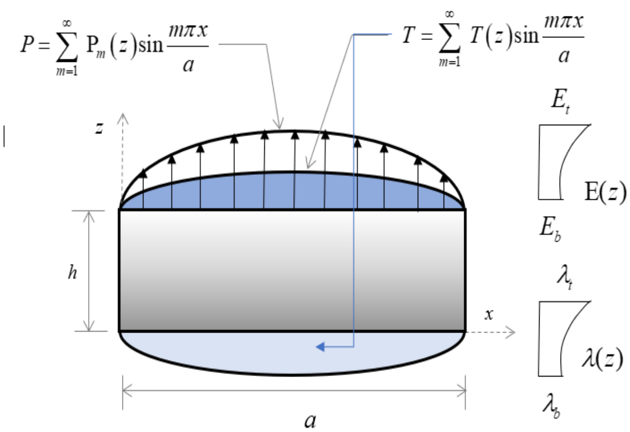

Fig. 1. FG laminate subjected to thermal &/or mechanical loading

3 SEMI-ANALYTICAL 2D HEAT CONDUCTION FORMULATION

The use of FG materials is primarily in situations where large temperature fields are experiencing on the structure, and hence, accurate determination of structural responses is of the utmost importance. In this section, the closed-form formulation for the 2D heat conduction equation has discussed. A thermal load and heat flux, as defined in (3) assumed with only known temperature value at the top and bottom of the laminate surface $\left(T = T_b \text{ at } z = 0 \text{ and } T = T_t \text{ at } z = h\right)$.

$$T(x,z) = \sum_{m=1}^{\infty} T(z) \sin \frac{m\pi x}{a} \text{ and}$$
$$q_z(x,z) = \sum_{m=1}^{\infty} q_z(z) \sin \frac{m\pi x}{a} \tag{3}$$

A governing two-dimensional (2D) steady-state heat conduction equation without internal heat generation is,

$$\lambda(z) \frac{\partial^2 T(x,z)}{\partial x^2} + \lambda(z) \frac{\partial^2 T(x,z)}{\partial z^2} = 0 \tag{4}$$

According to Fourier's law of heat conduction, heat flux in direction x and z is given by,

$$q_x(x,z) = -\lambda(z) \frac{\partial T(x,z)}{\partial x} ; q_z(x,z) = -\lambda(z) \frac{\partial T(x,z)}{\partial z} \tag{5}$$

where, q_i = heat flux along x and z-axis (i = x, z) in Wm^{-2}

International Journal Of Scientific & Engineering Research, Volume 10, Issue 12, December-2019
ISSN 2229-5518

And, with the assumption, that amount of heat remains in the element due to heat flow is zero, the equilibrium equation in 2D,

$$\frac{\partial q_x(x,z)}{\partial x}+\frac{\partial q_z(x,z)}{\partial z}=0 \tag{6}$$

Now, two variables viz. heat flux (q_z) and temperature field (T) are assumed as a primary variable. By using algebraic manipulation of the (5) and (6), a set of PDEs involving only two primary variables T and q_z obtained as follows.

$$\frac{\partial T(x,z)}{\partial z}=-\frac{1}{\lambda(z)}q_z(x,z)\ ;\ \frac{\partial q_z(x,z)}{\partial z}=-\lambda(z)\frac{\partial^2 T(x,z)}{\partial x^2} \tag{7}$$

By Substituting (3) and its derivatives into (7), the following set of the first-order ODE obtain as

$$\frac{dT_m(z)}{dz}=\frac{-1}{\lambda(z)}q_{zm}(z) \qquad \frac{dq_{zm}(z)}{dz}=-\lambda(z)\frac{m^2\pi^2}{a^2}T_m(z) \tag{8}$$

Equation (8) represents the governing two-point BVP in ODE's in the domain $0\le z\le h$ with known temperatures at the top and bottom surface of a laminate.

4 SEMI-ANALYTICAL 2D STRESS ANALYSIS FORMULATION

From the basic linear theory of elasticity, two-dimensional (2D) strain-displacement relationship, equations of equilibrium and constitutive relations in the thermo-elastic environment can be written as,

$$\varepsilon_x(x,z)=\frac{\partial u(x,z)}{\partial x}\ ;\ \varepsilon_z(x,z)=\frac{\partial w(x,z)}{\partial z}\ ;$$
$$\gamma_{xz}(x,z)=\frac{\partial u(x,z)}{\partial z}+\frac{\partial w(x,z)}{\partial x} \tag{9}$$

$$\frac{\partial \sigma_x(x,z)}{\partial x}+\frac{\partial \tau_{xz}(x,z)}{\partial z}+B_x=0$$
$$\frac{\partial \tau_{zx}(x,z)}{\partial x}+\frac{\partial \sigma_z(x,z)}{\partial z}+B_z=0 \tag{10}$$

and,

$$\begin{Bmatrix}\sigma_x(x,z)\\ \sigma_z(x,z)\\ \tau_{xz}(x,z)\end{Bmatrix}^i=\begin{pmatrix}C_{11} & C_{12} & 0\\ C_{12} & C_{22} & 0\\ 0 & 0 & C_{33}\end{pmatrix}^i\begin{Bmatrix}\varepsilon_x(x,z)-\alpha(z)T\\ \varepsilon_z(x,z)-\alpha(z)T\\ \gamma_{xz}(x,z)\end{Bmatrix}^i \tag{11}$$

Here $\alpha(z)T$ are the free thermal strains that arise due to temperature variation and B_x, B_z are the body forces per unit volume in x and z directions, respectively. These body forces are to neglect in the numerical investigation for the sake of simplicity. Material coefficients C_{ij} are the elastic constants derived by setting $\varepsilon_y=0$ and $\sigma_y=0$ in 3D material stiffness matrix for plane–strain and plane stress conditions, respectively. The reduced material ratios, C_{ij} for plane stress condition, are,

$$C_{11}=\frac{E(z)}{(1-\upsilon^2)};C_{12}=C_{21}=\frac{\upsilon E(z)}{(1-\upsilon^2)};C_{22}=\frac{E(z)}{(1-\upsilon^2)}$$

And C_{ij} for the plane-strain state are,

$$C_{11}=\frac{E(z)(1-\upsilon^2)}{(1-3\upsilon^2-2\upsilon^3)};C_{22}=\frac{E(z)(1-\upsilon^2)}{(1-3\upsilon^2-2\upsilon^3)};$$
$$C_{12}=C_{21}=\frac{E(z)(\upsilon+\upsilon^2)}{(1-3\upsilon^2-2\upsilon^3)};C_{33}=G_{13}$$

The above (9), (10) and (11) have a total of eight unknowns $u,\ w,\ \varepsilon_x,\ \varepsilon_z,\ \gamma_{xz},\ \sigma_x,\ \sigma_z,\ \tau_{xz}$ in eight equations. After a simple algebraic manipulation of the above-obtained sets of equations, a collection of PDEs involving only four dependent variables $u,\ w,\ \sigma_z$ and τ_{xz} obtained as follows.

$$\frac{\partial u(x,z)}{\partial z}=\frac{\tau_{zx}(x,z)}{C_{33}}-\frac{\partial w(x,z)}{\partial x}$$
$$\frac{\partial w(x,z)}{\partial z}=\frac{1}{C_{22}}\left[\sigma_z(x,z)-C_{21}\frac{\partial u(x,z)}{\partial x}+\alpha(z)T(x,z)(C_{21}+C_{22})\right] \tag{12}$$
$$\frac{\partial \tau_{zx}(x,z)}{\partial z}=\left[-C_{11}+\left(\frac{C_{12}C_{21}}{C_{22}}\right)\right]\frac{\partial^2 u(x,z)}{\partial x^2}-\frac{C_{12}}{C_{22}}\frac{\partial \sigma_z(x,z)}{\partial x}$$
$$-\left[\left(\frac{C_{12}C_{21}}{C_{22}}-C_{11}\right)\alpha(z)\right]\frac{\partial T(x,z)}{\partial x}-B_x\frac{\partial T(x,z)}{\partial x}$$
$$\frac{\partial \sigma_z(x,z)}{\partial z}=-\frac{\partial \tau_{xz}(x,z)}{\partial x}-B_z\frac{\partial T(x,z)}{\partial x}$$

And, a secondary dependent variable, $\sigma_x(x,z)$ can be expressed as a function of the initial set of variables as follows.

$$\sigma_x(x,z)=C_{11}\frac{\partial u(x,z)}{\partial x}+C_{12}\frac{\partial w(x,z)}{\partial z}-(C_{11}+C_{12})\alpha(z)T(x,z) \tag{13}$$

The above PDE's defined by (12) can reduce to a coupled first-order ODEs by using Fourier trigonometric series expansion. Where primary variables satisfying exactly the simply (diaphragm) support end conditions at $x=0$ and a as follows,

$$u(x,z)=\sum_{m=1}^{\infty}u_m(z)\cos\left(\frac{m\pi x}{a}\right),\ w(x,z)=\sum_{m=1}^{\infty}w_m(z)\sin\left(\frac{m\pi x}{a}\right) \tag{14}$$

and from the fundamental relations of the theory of elasticity, it can be shown that,

$$\tau_{xz}(x,z)=\sum_{m=1}^{\infty}\tau_{xzm}(z)\cos\frac{m\pi x}{l} \qquad \sigma_z(x,z)=\sum_{m=1}^{\infty}\sigma_{zm}(z)\sin\frac{m\pi x}{l} \tag{15}$$

Further, applied transverse loading on the top of the laminate and temperature variation along the x-direction is also express in sinusoidal form as,

$$P(x,z)=\sum_{m=1}^{\infty}P_m(z)\sin\frac{m\pi x}{l}\ \ and\ \ T(x,z)=\sum_{m=1}^{\infty}T(z)\sin\frac{m\pi x}{l} \tag{16}$$

Substituting Equation (14), (15) and (16) and its derivatives into (12), the following ordinary differential equations (ODEs) has obtained as

International Journal Of Scientific & Engineering Research, Volume 10, Issue 12, December-2019
ISSN 2229-5518

$$\frac{du_m(z)}{dz}=\left(-\frac{m\pi}{a}\right)w_m(z)+\left(\frac{1}{C_{33}}\right)\tau_{xzm}(z)$$
$$\frac{dw_m(z)}{dz}=\left(\frac{C_{21}}{C_{22}}\frac{m\pi}{a}\right)u_m(z)+\left(\frac{1}{C_{22}}\right)\sigma_{zm}(z)+\left(\frac{C_{21}+C_{22}}{C_{22}}\right)\alpha(z)T(z)$$
$$\frac{d\tau_{xzm}(z)}{dz}=\left(\frac{C_{12}C_{21}}{C_{22}}-C_{11}\right)\left(\frac{m^2\pi^2}{a^2}\right)u_m(z)-\left(\frac{C_{12}}{C_{22}}\frac{m\pi}{a}\right)\sigma_{zm}(z)$$
$$-\left(\frac{C_{12}C_{21}}{C_{22}}-C_{11}\right)\left(\frac{m\pi}{a}\right)\alpha(z)T(z)-B_x(x,z)$$
$$\frac{d\sigma_{zm}(z)}{dz}=\left(\frac{m\pi}{l}\right)\tau_{xzm}(z)-B_z(x,z) \quad (17)$$

(17) represents the governing two-point BVP in ODE's in the domain $0 \le z \le h$ with stress components known at the top and bottom surfaces of a beam/plate.

The basic approach to numerical integration of the BVP defined in Equation (8), (17) and the associated boundary conditions when it contains no boundary layer effects. It is to transform the given BVP into a set of IVP's one non-homogeneous and $n/2$ homogeneous, here n equal to 2 and 4 for heat conduction formulation and stress analysis formulation, respectively. Table 1 and Table 2 detailed the transformation of BVP to IVPs for thermal and stress analysis, respectively. Further, the solutions of defined BVP (. 8 and 17) have obtained by forming a linear combination of one non-homogeneous and $n/2$ homogeneous solution to satisfy the boundary conditions $z=h$. These give rise to a system of $n/2$ linear algebraic equations, the answer of which determines the unknown $n/2$ components at the starting edge $z=0$. Then a final numerical integration of (8), (17) produces the desired results. The fourth-order Runge-Kutta method is used here for numerical combinations. Displacements, stresses, and temperature boundary conditions have detailed in Table 3.

5 NUMERICAL STUDIES

Computer codes have developed by incorporating the present formulation to determine the exact temperature variation through the thickness of FG laminates and also for thermomechanical stress analysis of FG laminates. Semi-analytical solutions of FG laminate (Material Set 1: Table 3) subjected to only mechanical loading under plane-stress conditions for elasticity has first compared with available solutions in the literature for validation purpose and tabulated in Table 4 and found to be very close in agreement with them. For numerical investigations in the present study, the reference temperature at the bottom and the top surface of the FG laminate are assuming as 200 C and 3000 C, respectively. Three material combinations listed in Table 3 have considered for investigating the effect of material gradation on the temperature distribution through the thickness of FG laminate and for stress analysis. This study had carried out when FG laminate is subject to only thermal loading and thermomechanical loading. Based on the convergence studies, around 20 to 30 steps have used through the thickness of laminate for numerical integration. Distribution of temperature field along the depth of FG laminate for all material sets has obtained by the semi-analytical approach for aspect ratios (s) 5, 10, 20, and 50, and the results of the same indicated in fig. 2. The exponential distribution of temperature filed has also presented in the same figure and compared. It is observed from fig. 2 that there is a considerable difference in temperature field obtained by solving the heat-conduction equation when compared with the assumed exponential temperature field. It is for material set 1, which proves the sensitivity of material gradation of FG material for temperature distribution. However, the effect of aspect ratio on the temperature field for FG materials is not observing in the present investigation. It is to note that for plane strain conditions of elasticity, temperature variation through the thickness of laminate has remained the same. It is because heat conduction formulation is independent of materials Young's and shear modulus and Poisson's ratio.

Further, stress analysis performed by using a semi-analytical approach when the laminate is subject to only the thermal loads for both plane-stress and plane-strain conditions of elasticity. All three material sets have considered here for aspect ratio (s) 5, 10, 20, and 50. Following normalizations coefficients have used here for a uniform comparison of the results,

$$s=\frac{a}{h} \quad \bar{u}_n=\frac{10u_n}{h\alpha_b T_b s^2} \quad \bar{w}_n=\frac{10w_n}{h\alpha_b T_b s^2} \quad \bar{\sigma}_x=\frac{\sigma_x}{E_b\alpha_b T_b} \quad \bar{\tau}_{xz}=\frac{\tau_{xz}s^2}{E_b\alpha_b T_b} \quad (18)$$

In which bar over the variables defines its normalized value. Response for in-plane displacement $(\bar{u})$, transverse displacement $(\bar{w})$, in-plane normal stress $(\bar{\sigma}_x)$, and transverse shear stress $(\bar{\tau}_{xz})$ obtained for specific temperature field [Model 1] as well as for exponential varied temperature field [Model 2] have documented in Table 5 and 6 for plane-stress and plane strain conditions, respectively. Through thickness profile of in-plane displacement $(\bar{u})$, transverse displacement $(\bar{w})$, in-plane normal stress $(\bar{\sigma}_x)$, and transverse shear stress $(\bar{\tau}_{xz})$ have compared between responses obtained from Model 1 and Model 2 for aspect ratio (s) 5 in fig. 3 to fig. 5 for material sets 1, 2, and 3, respectively. Tentatively the same patterns of profiles for all parameters through the thickness of a laminate obtained by Model 1 and Model 2 have observed in fig. 3 to fig. 5. However, considerable differences in maximum and minimum

International Journal Of Scientific & Engineering Research, Volume 10, Issue 12, December-2019
ISSN 2229-5518

numerical values have noted for material set 1 and 2 (fig. 3 and 4), whereas, for set 3, no significant difference in variation, as well as their numerical values, have been noted (fig. 5).

From Tables 5 and 6, it has pointed out that stress analysis for exponential temperature field (Model 2) overestimate in-plane displacement $(\bar{u})$ and transverse displacement $(\bar{w})$. These results are more than 22% and 11%, respectively, when compared with Model 1 for material set 1. Whereas underestimation of values of in-plane normal stress $(\bar{\sigma}_x)$ and transverse shear stress $(\bar{\tau}_{xz})$ by more than 50% and 45%, respectively, for set 1 when both Model 1 and Model 2 results have compared. It has even observed for thin laminate (s= 50). Further, for set 2 and set 3, no significant difference in magnitude is to see for in-plane displacement $(\bar{u})$ and transverse displacement $(\bar{w})$ observed. However, underestimation of in-plane normal stress $(\bar{\sigma}_x)$ and transverse shear stress $(\bar{\tau}_{xz})$ has noted nearly 25% and 20% for material set 2, and almost 11% and 8% for content set 3.

Here, stress analysis performed by using a semi-analytical approach when the laminate is subject to thermal loading and transverse loading on the top surface of laminate for both plane-stress and plane-strain conditions of elasticity for all three material sets and aspect ratio (s) 5, 10, 20 and 50. Following normalized coefficients have used here for the comparison of the results.

$$s=\frac{a}{h} \quad \bar{u}=\frac{u}{h\alpha_b T_b s^3};\ \bar{w}=\frac{w}{h\alpha_b T_b s^4};\ \bar{\sigma}_x=\frac{\sigma_x}{1000 P_0 \alpha_b T_b s^2};\ \bar{\tau}_{xz}=\frac{10000\tau_{xz}}{P_0\alpha_b T_b s} \tag{19}$$

in which bar over the variables defines its normalized value.

Response for in-plane displacement $(\bar{u})$, transverse displacement $(\bar{w})$, in plane normal stress, $(\bar{\sigma}_x)$ and transverse shear stress $(\bar{\tau}_{xz})$ obtained from Model 1 and Model 2 have documented in Tables 7 and 8 for plane-stress and plane strain conditions, respectively. Through thickness variation of in-plane displacement $(\bar{u})$, transverse displacement $(\bar{w})$, in-plane normal stress $(\bar{\sigma}_x)$, and transverse shear stress $(\bar{\tau}_{xz})$ have compared between responses obtained from Model 1 and Model 2 for aspect ratio (s) 5 in fig. 6 to fig. 8 for material set 1,2 and 3, respectively. However, when the laminate is subject to thermal loading along with mechanical loading, no significant differences have seen for all parameters in the responses obtained from Model 1 and Model 2. These may be due to the neutralizing the overall effect of thermal loading by mechanical loading. However, an intensity of mechanical loading effects has not investigated in the present studies.

6 CONCLUDING REMARKS

Semi-analytical formulations based on a two-point boundary value problem governed by a set of coupled first-order ordinary differential equations (ODEs) and free from simplified assumptions along the thickness of laminates for heat conduction equation and stress analysis have discussed in this paper. A comparison between exponential varied temperature fields along the depth of the laminate and temperature field obtained through heat conduction solutions have documented. These are recorded for different material sets and for various aspect ratios ranging from thick to thin laminates, which proves the sensitivity of the determination of the exact temperature field before stress analysis. However, the effect of aspect ratio is not observing in the present studies on the thermal field through the laminate thickness.

Further, stress analyses performed and document for both thermal and thermomechanical loading under plane-stress and plane-strain conditions of elasticity. Considerable differences have been noted down during stress analysis for the thermal load on various parameters from displacement and stress groups. It has also observed that no significant difference recorded for stress analysis with thermomechanical loading.

REFERENCES

[1] V. Sankar, An elasticity solution for functionally graded beams, Composites Science and Technology, 689 – 696, 2001.
[2] Z. Zhong, T. Yu, Analytical solution of a cantilever functionally graded beam, Composites Science and Technology, 481 – 488, 2007.
[3] M. A. Benatta, I. Mechab, A. Tounsi, E. A. Adda Bedia, Static analysis of functionally graded short beams including warping and shear deformation effects, Computational Materials Science, 2008.
[4] S. S. Pendhari, T. Kant, Y. M. Desai, C. V. Subbaiah, On the deformation of functionally graded narrow beams under transverse loads, International Journal of Mechanics and Materials in Design, vol. 6, 269 – 282, 2010.
[5] H. T. Thai, and T. P. Vo, Bending and free vibration of functionally graded beams using various higher-order shear deformation beam theories, International Journal of Mechanical Sciences, vol. 62, 57 – 66, 2012.
[6] M. Şimşek, and J. N. Reddy, Bending and vibration of functionally graded microbeams using a new higher-order beam theory and the modified couple stress theory, International Journal of Engineering Science, vol. 64, 37 – 53, 2013.
[7] N. Noda, Thermal stresses in functionally graded materials, Journal of Thermal Stresses, vol. 22, 477-512, 1999.
[8] V. Sankar, J. T. Tzeng, Thermal-Stress analysis of functionally graded beams, American Institute of Aeronautics & Astronautics, vol. 40, 1228-1232, 2002.
[9] A. Carpinteri, M. Paggi, Thermo-elastic mismatch in nonhomogeneous beams, Journal of Engineering Mathematics, vol. 61, 371–384, 2008.

International Journal Of Scientific & Engineering Research, Volume 10, Issue 12, December-2019
ISSN 2229-5518

[10] R. Kadoli, K. N. Akhtar, Ganesan, Static analysis of functionally graded beams using higher-order shear deformation theory, Applied Mathematical Modelling, vol. 32, 2509 – 2525, 2008.

[11] N. Wattanasakulpong, B. G. Prusty, D. W. Kelly, Thermal buckling and elastic vibration of third-order shear deformable functionally graded beams, International Journal of Mechanical Sciences, vol. 53, 734 – 743, 2011.

[12] M. Lezgy-Nazargah Fully coupled thermo-mechanical analysis of bi-directional FGM beams using NURBS isogeometric finite element approach, Aerospace Science and Technology, vol. 45, 154 – 164, 2015.

[13] N. A. Apetre, B. V. Sankar, D. R. Ambur, Analytical modeling of sandwich beams with functionally graded core, Journal of Sandwich Structures and Materials, 2008.

[14] A. Chakraborty, S. Gopalakrishnan, J. N. Reddy, A new beam finite element for the analysis of functionally graded materials, International Journal of Mechanical Sciences, vol. 45, 519 – 539, 2003.

[15] E. Carrera, M. Petrolo, P. Nali, Unified formulation applied to free vibrations finite element analysis of beams with arbitrary section, Shock and Vibration, vol. 502, 485 – 502, 2011.

[16] H. Wang, Q. H. Qin, Meshless approach for thermo-mechanical analysis of functionally graded materials, Engineering Analysis with Boundary Elements, vol. 32, 704-712, 2008.

[17] Y. Kiani, M. R. Eslami, Thermal buckling analysis of functionally graded material beams, International Journal of Mechanics and Materials in Design, vol. 6, 229 – 238, 2010.

[18] G. Giunta, D. Crisafulli, S. Belouettar, E. Carrera, A thermo-mechanical analysis of functionally graded beams via hierarchical modeling, Composite Structures, vol. 95, 676 – 690, 2013.

[19] L. V. Kantrovich, V. I. Krylov, Approximate Methods of Higher Analysis, 3rd Edition, Noordhoff, Groningen, 304-327, 1958.

International Journal Of Scientific & Engineering Research, Volume 10, Issue 12, December-2019
ISSN 2229-5518

TABLE 1

TRANSFORMATION OF BVP INTO IVP'S FOR THERMAL ANALYSIS

Integration No.	Bottom edge $(z=0)$		Top edge $(z=h)$	
	$T(z)$	$q_z(z)$	$T(z)$	$q_z(z)$
1	Known	0 (assumed)	M_{11}	M_{21}
2	0 (assumed)	1 (assumed)	M_{12}	M_{22}
3 (Final)	$T(0)$ (known)	$K1$	$T(h)$ (known)	$q_z(h)$

TABLE 2

TRANSFORMATION OF BVP INTO IVP'S FOR STRESS ANALYSIS

Integration No.	Bottom edge $(z=0)$				Top edge $(z=h)$				Load/Temp. Term
	u	w	τ_{xz}	σ_z	u	w	τ_{xz}	σ_z	
1	0 (assumed)	0 (assumed)	0 (known)	0 (known)	Y_{11}	Y_{21}	Y_{31}	Y_{21}	Include
2	1 (assumed)	0 (assumed)	0 (assumed)	0 (assumed)	Y_{12}	Y_{22}	Y_{32}	Y_{42}	Exclude
3	0 (assumed)	1 (assumed)	0 (assumed)	0 (assumed)	Y_{13}	Y_{23}	Y_{33}	Y_{34}	Exclude
4 (Final)	X_1	X_2	0 (known)	0 (known)	$u(h)$	$w(h)$	0 (known)	0 (known)	Include

TABLE 3

MATERIAL PROPERTIES

Set	Material Properties
a	At bottom, $z=0 \Rightarrow$ Aluminium : $E=70\ GPa$ $\mu=0.3$ $\lambda=204\ K^{-1}$ $\alpha=23\times10^{-6}\ W_m^{-1}K^{-1}$ At top, $z=h \Rightarrow$ Zirconia : $E=151\ GPa$ $\mu=0.3$ $\lambda=2.09\ K^{-1}$ $\alpha=10\times10^{-6}\ W_m^{-1}K^{-1}$
b	At bottom, $z=0 \Rightarrow$ Aluminium : $E=70\ GPa$ $\mu=0.3$ $\lambda=204K^{-1}$ $\alpha=23\times10^{-6}\ W_m^{-1}K^{-1}$ At top, $z=h \Rightarrow$ Alumina : $E=380\ GPa$ $\mu=0.326$ $\lambda=10.40K^{-1}$ $\alpha=7.4\times10^{-6}\ W_m^{-1}K^{-1}$
c	At bottom, $z=0 \Rightarrow$ Monel : $E=227.24\ GPa$ $\mu=0.3$ $\lambda=25\ K^{-1}$ $\alpha=15\times10^{-6}\ W_m^{-1}K^{-1}$

International Journal Of Scientific & Engineering Research, Volume 10, Issue 12, December-2019
ISSN 2229-5518

At top,	$z = h \Rightarrow$ Zirconia	: $E = 151\ GPa$	$\mu = 0.3$	λ=2.09 K^{-1}	$\alpha = 10 \times 10^{-6}\ W_m^{-1} K^{-1}$

Ref. Kadoli et al. [11]

International Journal Of Scientific & Engineering Research, Volume 10, Issue 12, December-2019
ISSN 2229-5518

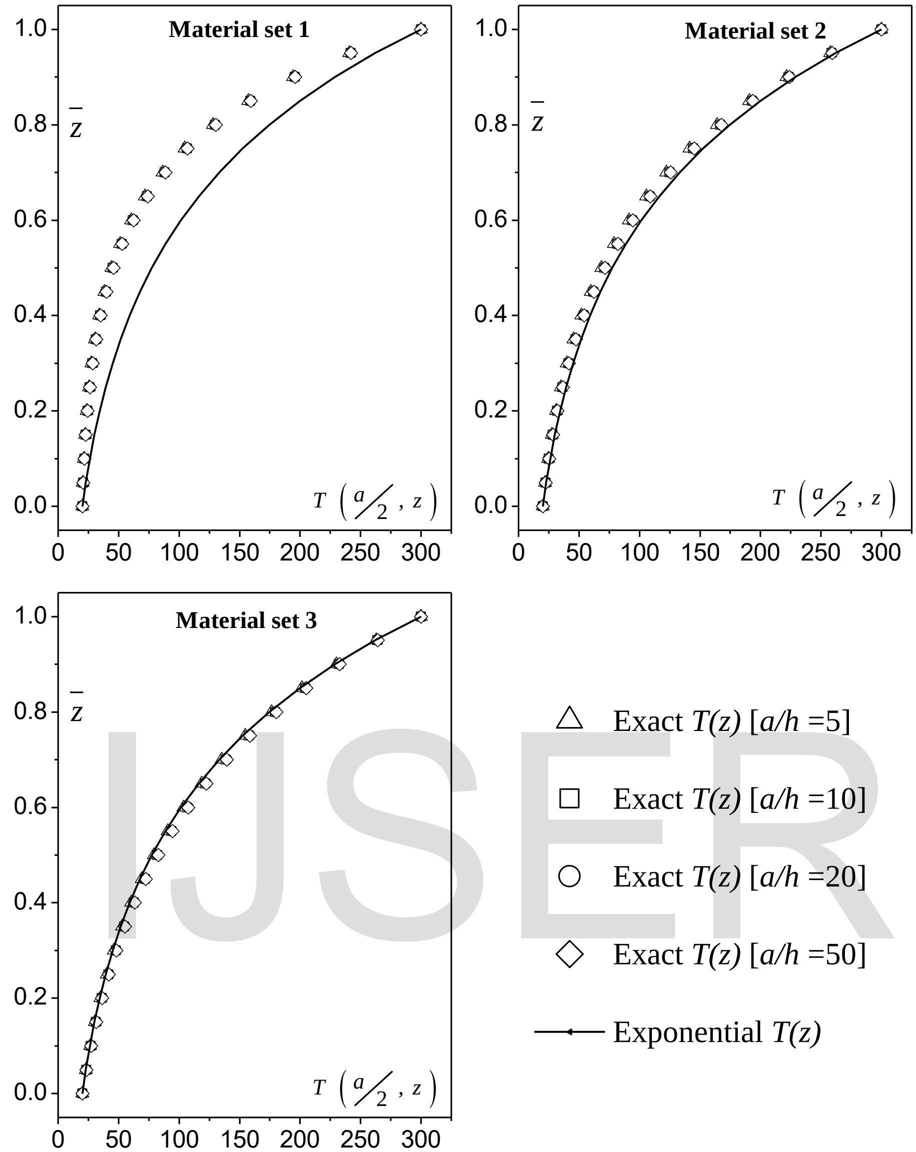

Fig. 2. Comparison of through thickness exact and exponential temperature variations.

International Journal Of Scientific & Engineering Research, Volume 10, Issue 12, December-2019
ISSN 2229-5518

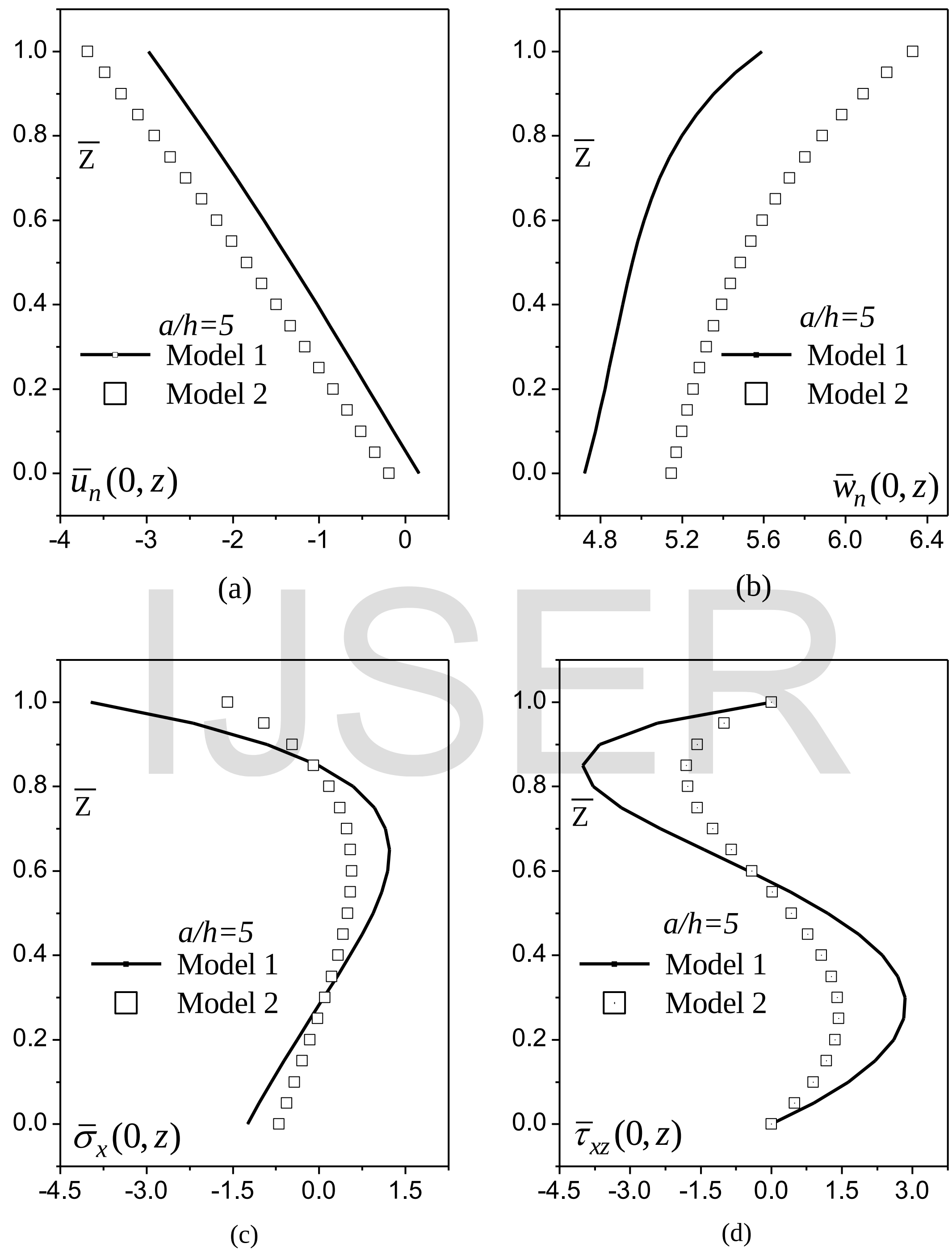

Fig. 3. The Variation of normalized (a) in-plane displacement $\bar{u}_n$ (b) transverse displacement $\bar{w}_n$ (c) in-plane normal stress $\bar{\sigma}_x$ (d) transverse shear stress $\bar{\tau}_{xz}$ through thickness of FG laminate under plane-stress condition subjected to the thermal load, $T(x,z) = T(z)\sin {\pi x}/{a}$ (Material set 1).

International Journal Of Scientific & Engineering Research, Volume 10, Issue 12, December-2019
ISSN 2229-5518

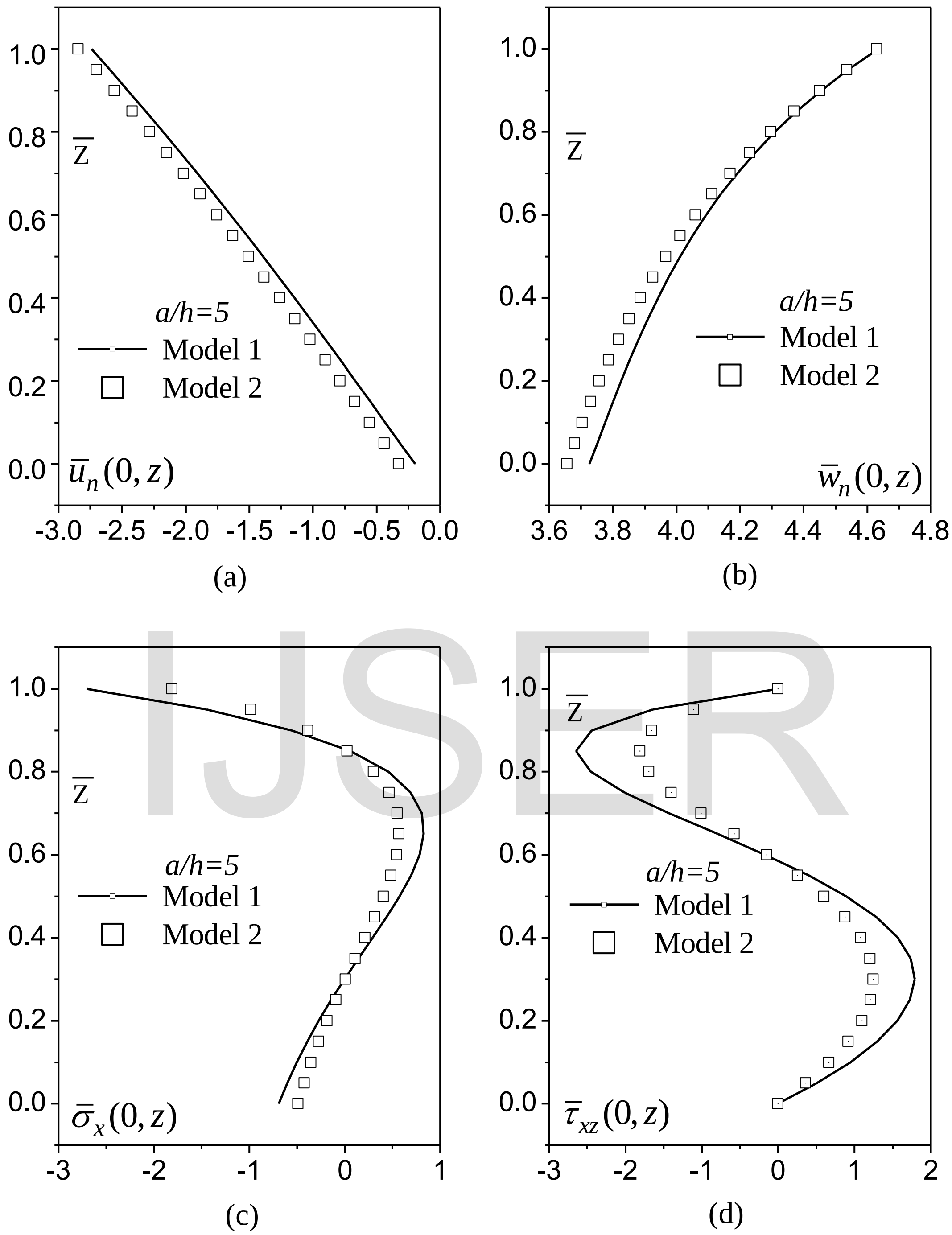

Fig. 4. The Variation of normalized (a) in-plane displacement $\bar{u}_n$ (b) transverse displacement $\bar{w}_n$ (c) in-plane normal stress $\bar{\sigma}_x$ (d) transverse shear stress $\bar{\tau}_{xz}$ through thickness of FG laminate under plane-stress condition subjected to the thermal load, $T(x,z) = T(z)\sin {\pi x}/{a}$ (Material set 2).

International Journal Of Scientific & Engineering Research, Volume 10, Issue 12, December-2019
ISSN 2229-5518

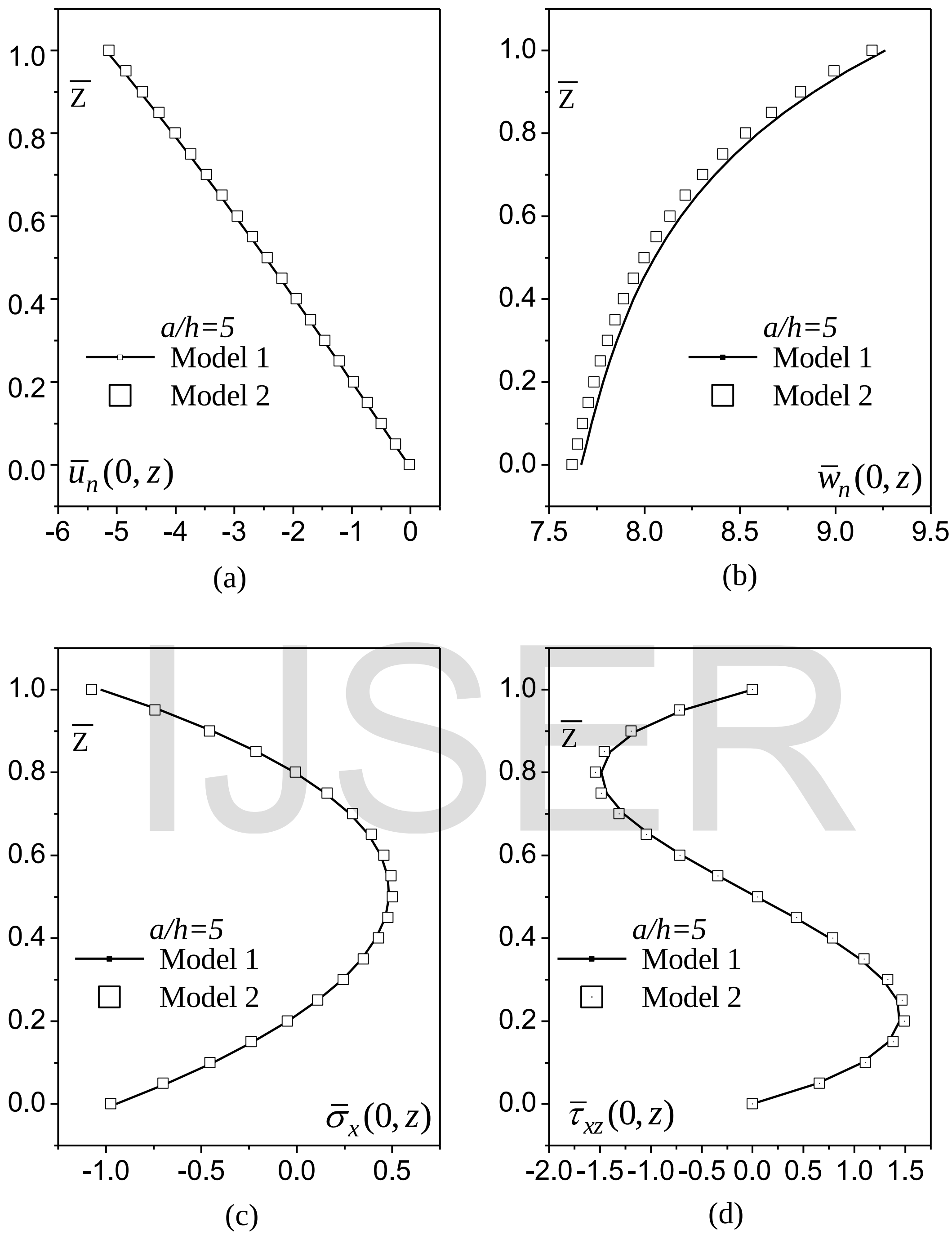

Fig. 5. The Variation of normalized (a) in-plane displacement $\overline{u}_n$ (b) transverse displacement $\overline{w}_n$ (c) in-plane normal stress $\overline{\sigma}_x$ (d) transverse shear stress $\overline{\tau}_{xz}$ through thickness of FG laminate under plane-stress condition subjected to the thermal load, $T(x,z) = T(z)\sin \pi x/a$ (Material set 3).

International Journal Of Scientific & Engineering Research, Volume 10, Issue 12, December-2019
ISSN 2229-5518

TABLE 4

NORMALIZED TRANSVERSE DISPLACEMENTS $(\bar{u})$ AND STRESSES $(\bar{\sigma}_x, \bar{\tau}_{xz})$ OF FG LAMINATE SUBJECTED TO ONLY MECHANICAL LOADING PLANE STRESS CONDITION

s	Source	$\bar{w}_n\left(a/2, \max\right)$	$\bar{\tau}_{xz}\left(0, \max\right)$	$\bar{\sigma}_x\left(a/2, 0\right)$
5	Present Analysis	19.919	0.480	0.797
	Sankar (2001)	19.779	0.480	0.797
10	Present Analysis	18.615	0.481	0.787
	Sankar (2001)	18.568	0.481	0.787
50	Present Analysis	18.198	0.481	0.783
	Sankar (2001)	18.196	0.481	0.784

International Journal Of Scientific & Engineering Research, Volume 10, Issue 12, December-2019
ISSN 2229-5518

TABLE 5

NORMALIZED IN-PLANE AND TRANSVERSE DISPLACEMENTS $(\bar{u},\bar{w})$ AND STRESSES $(\bar{\sigma}_x,\bar{\tau}_{xz})$ OF FG LAMINATE UNDER THERMAL LOADING FOR MATERIAL SET 1, 2 AND 3 FOR PLANE STRESS CONDITION

s	Source	$\bar{u}\ (0, h \& 0)$		$\bar{w}\left(a/2, \max\right)$	$\bar{\tau}_{xz}(0, \max)$	$\bar{\sigma}_x\left(a/2, h \& 0\right)$	
Material Set 1							
5	Model 1	-2.980	0.157	5.589	2.841	-3.972	-1.247
	Model 2	-3.683	-0.192	6.329	1.428	-1.588	-0.698
10	Model 1	-1.483	0.913	5.160	5.850	-4.021	-1.287
	Model 2	-1.816	-0.072	5.746	3.175	-1.756	-0.774
20	Model 1	-0.740	0.047	5.052	11.786	-4.034	-1.297
	Model 2	-0.905	-0.330	5.601	6.514	-1.799	-0.793
50	Model 1	-0.296	0.019	5.021	29.524	-4.037	-1.300
	Model 2	-0.361	-0.012	5.560	16.399	-1.810	-0.797
Material Set 2							
5	Model 1	-2.742	-0.198	4.635	1.787	-2.707	-0.689
	Model 2	-2.847	-0.326	4.635	1.244	-1.812	-0.489
10	Model 1	-1.368	-0.091	4.213	3.701	-2.759	-0.714
	Model 2	-1.407	-0.138	4.192	2.892	-2.096	-0.566
20	Model 1	-0.683	-0.045	4.105	7.465	-2.773	-0.720
	Model 2	-0.701	-0.066	4.082	5.990	-2.168	-0.585
50	Model 1	-0.273	-0.018	4.075	18.710	-2.777	-0.722
	Model 2	-0.280	-0.026	4.052	15.120	-2.188	-0.591
Material Set 3							
5	Model 1	-5.184	-0.034	9.261	1.445	-1.028	-0.947
	Model 2	-5.132	-0.017	9.193	1.492	-1.073	-0.974
10	Model 1	-2.585	-0.006	8.477	2.987	-1.041	-0.980
	Model 2	-2.523	0.014	8.337	3.212	-1.149	-1.044
20	Model 1	-1.291	-0.002	8.277	6.025	-1.045	-0.989
	Model 2	-1.256	0.010	8.124	6.540	-1.168	-1.062
50	Model 1	-0.516	-0.001	8.221	15.098	-1.045	-0.991
	Model 2	-0.502	0.004	8.064	16.432	-1.173	-1.067

International Journal Of Scientific & Engineering Research, Volume 10, Issue 12, December-2019
ISSN 2229-5518

TABLE 6

NORMALIZED IN-PLANE AND TRANSVERSE DISPLACEMENTS $(\bar{u}, \bar{w})$ AND STRESSES $(\bar{\sigma}_x, \bar{\tau}_{xz})$ OF FG LAMINATE UNDER THERMAL LOADING FOR MATERIAL SET 1, 2 AND 3 FOR PLANE STRAIN CONDITION

s	Source	$\bar{u}\ (0, h \& 0)$		$\bar{w}\left(a/2, \max\right)$	$\bar{\tau}_{xz}(0, \max)$	$\bar{\sigma}_x\left(a/2, h \& 0\right)$	
				Material Set 1			
5	Model 1	-2.980	1.573	5.589	3.122	-4.364	-1.370
	Model 2	-3.683	-1.920	6.330	1.569	-1.745	-0.767
10	Model 1	-1.483	0.091	5.161	6.428	-4.419	-1.414
	Model 2	-1.817	-0.072	5.747	3.489	-1.930	-0.850
20	Model 1	-0740	0.047	5.052	12.951	-4.432	-1.426
	Model 2	-0.905	-0.330	5.601	7.158	-1.976	-0.871
50	Model 1	-0.296	0.019	5.022	32.444	-4.436	-1.429
	Model 2	-0.362	-0.013	5.561	18.022	-1.989	-0.877
				Material Set 2			
5	Model 1	-2.742	-0.198	4.635	1.999	-3.027	-0.771
	Model 2	-2.847	-0.326	4.631	1.392	-2.027	-0.546
10	Model 1	-1.368	-0.091	4.213	4.140	-3.087	-0.799
	Model 2	-1.407	-0.138	4.192	3.235	-2.345	-0.633
20	Model 1	-0.683	-0.045	4.105	8.351	-3.102	-0.806
	Model 2	-0.701	-0.066	4.082	6.701	-2.426	-0.655
50	Model 1	-0.273	-0.018	4.075	20.931	-3.106	-0.808
	Model 2	-0.280	-0.026	4.052	16.915	-2.448	-0.661
				Material Set 3			
5	Model 1	-5.184	-0.034	9.261	1.587	-1.130	-1.040
	Model 2	-5.132	-0.017	9.193	1.639	-1.179	-1.070
10	Model 1	-2.585	-0.006	8.477	3.282	-1.144	-1.077
	Model 2	-2.523	0.014	8.337	3.530	-1.262	-1.147
20	Model 1	-1.291	-0.002	8.277	6.620	-1.148	-1.087
	Model 2	-1.256	0.010	8.124	7.187	-1.283	-1.167
50	Model 1	-0.516	-0.001	8.221	16.591	-1.149	-1.089
	Model 2	-0.502	0.004	8.064	18.057	-1.289	-1.172

International Journal Of Scientific & Engineering Research, Volume 10, Issue 12, December-2019
ISSN 2229-5518

International Journal Of Scientific & Engineering Research, Volume 10, Issue 12, December-2019
ISSN 2229-5518

International Journal Of Scientific & Engineering Research, Volume 10, Issue 12, December-2019
ISSN 2229-5518

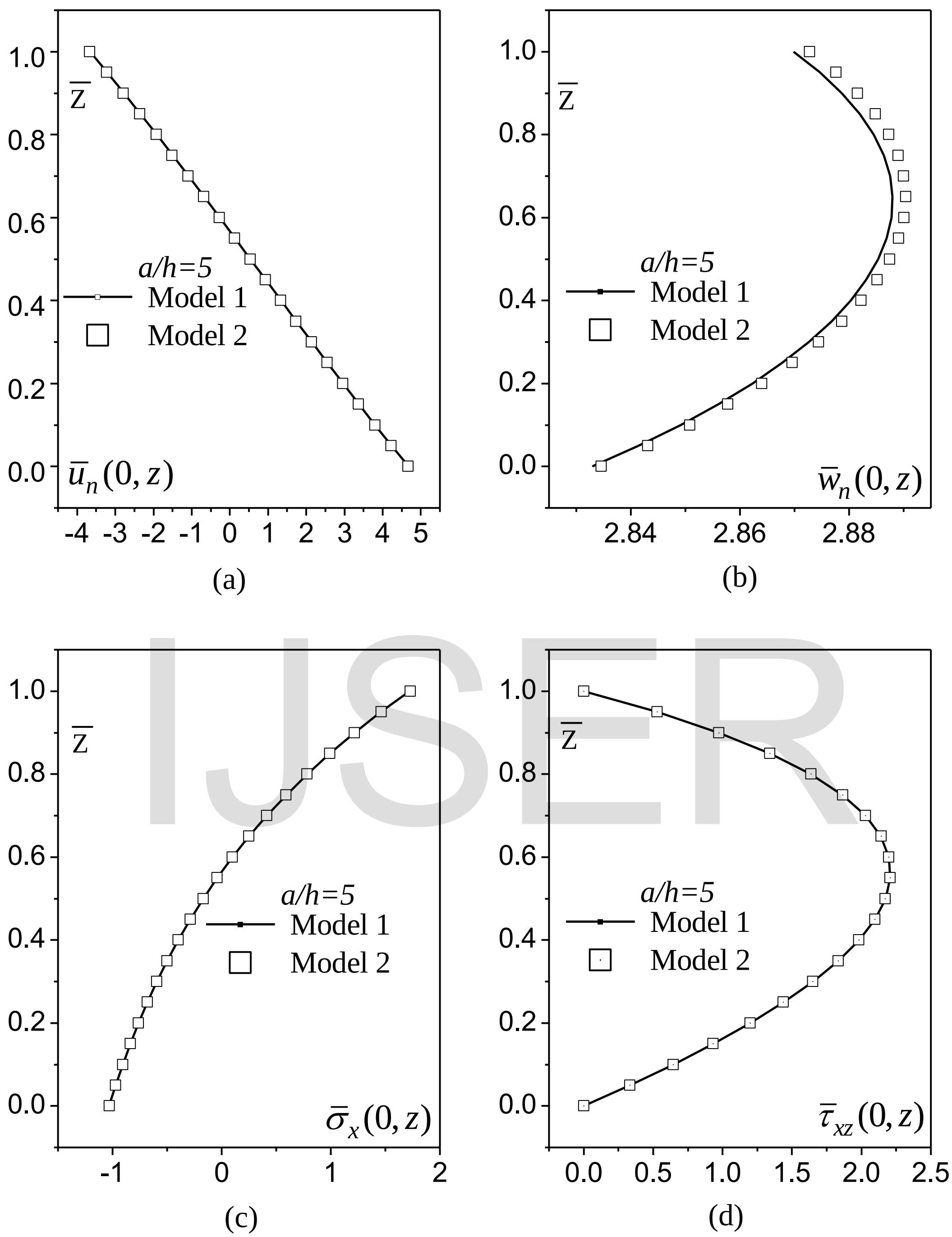

Fig. 6. The Variation of normalized (a) in-plane displacement $\overline{u}_n$ (b) transverse displacement $\overline{w}_n$ (c) in-plane normal stress $\overline{\sigma}_x$ (d) transverse shear stress $\overline{\tau}_{xz}$ through thickness of FG laminate under plane-stress condition subjected to thermomechanical load, (Material set 1).

International Journal Of Scientific & Engineering Research, Volume 10, Issue 12, December-2019
ISSN 2229-5518

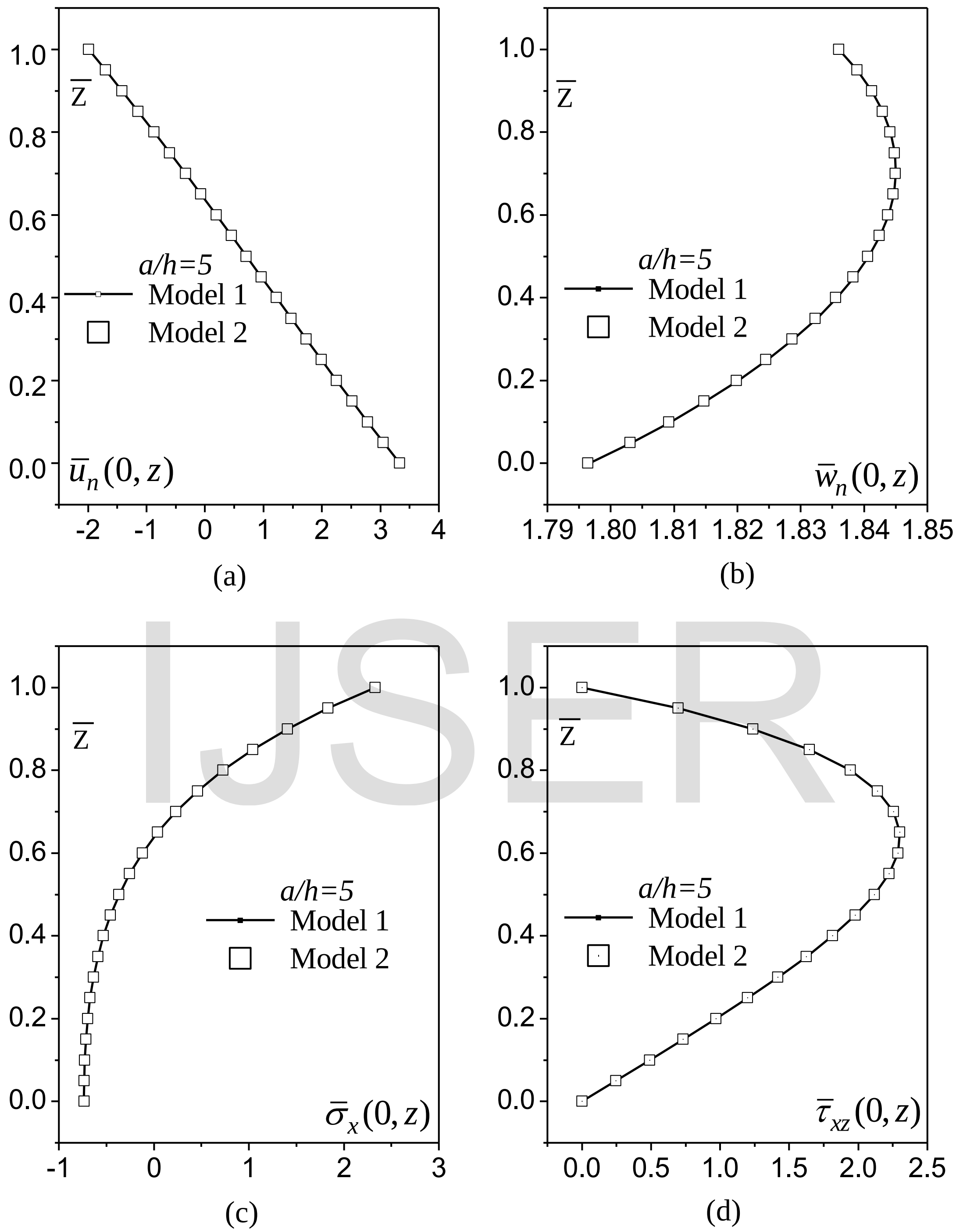

Fig. 7. The Variation of normalized (a) in-plane displacement $\overline{u}_n$ (b) transverse displacement $\overline{w}_n$ (c) in-plane normal stress $\overline{\sigma}_x$ (d) transverse shear stress $\overline{\tau}_{xz}$ through thickness of FG laminate under plane-stress condition subjected to thermomechanical load, (Material set 2).

International Journal Of Scientific & Engineering Research, Volume 10, Issue 12, December-2019
ISSN 2229-5518

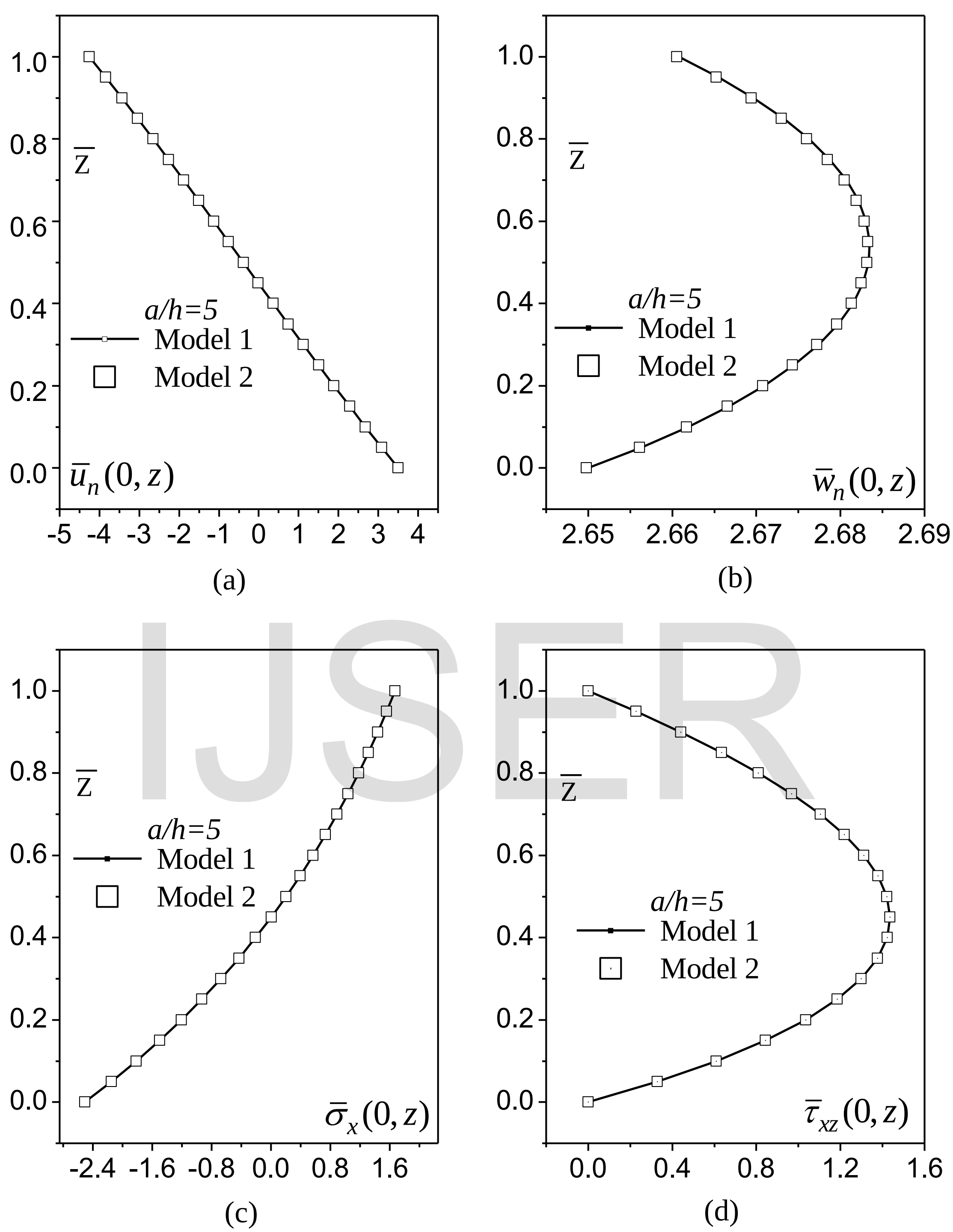

Fig. 8. The Variation of normalized (a) in-plane displacement $\bar{u}_n$ (b) transverse displacement $\bar{w}_n$ (c) in-plane normal stress $\bar{\sigma}_x$ (d) transverse shear stress $\bar{\tau}_{xz}$ through thickness of FG laminate under plane-stress condition subjected to thermomechanical load, (Material set 3).